Analysis of *Msx1*; *Msx2* double mutants reveals multiple roles for Msx genes in limb development

Yvan Lallemand, Marie-Anne Nicola*, Casto Ramos*,†, Antoine Bach‡, Cécile Saint Cloment and Benoît Robert§

Unité de Génétique Moléculaire de la Morphogenèse, Institut Pasteur, URA 2578 du CNRS, 25 rue du Dr Roux, 75724 Paris, Cedex 15, France

*These authors contributed equally to this work
†Present address: Depto de Biologia Celular, Facultad de Biologia, Av. Diagonal, 645, 08071 Barcelona, Spain
‡Present address: INSERM U679, Neurobiologie et Thérapeutique Expérimentale, Hôpital de la Salpêtrière, 47 boulevard de l'Hôpital, 75013 Paris, France
§Author for correspondence (e-mail: brobert@pasteur.fr)

Accepted 25 April 2005

Development 132, 3003-3014
Published by The Company of Biologists 2005
doi:10.1242/dev.01877

Summary

The homeobox-containing genes *Msx1* and *Msx2* are highly expressed in the limb field from the earliest stages of limb formation and, subsequently, in both the apical ectodermal ridge and underlying mesenchyme. However, mice homozygous for a null mutation in either *Msx1* or *Msx2* do not display abnormalities in limb development. By contrast, *Msx1; Msx2* double mutants exhibit a severe limb phenotype. Our analysis indicates that these genes play a role in crucial processes during limb morphogenesis along all three axes. Double mutant limbs are shorter and lack anterior skeletal elements (radius/tibia, thumb/hallux). Gene expression analysis confirms that there is no formation of regions with anterior identity. This correlates with the absence of dorsoventral boundary specification in the anterior ectoderm, which precludes apical ectodermal ridge formation anteriorly. As a result, anterior mesenchyme is not maintained, leading to oligodactyly. Paradoxically, polydactyly is also frequent and appears to be associated with extended Fgf activity in the apical ectodermal ridge, which is maintained up to 14.5 dpc. This results in a major outgrowth of the mesenchyme anteriorly, which nevertheless maintains a posterior identity, and leads to formation of extra digits. These defects are interpreted in the context of an impairment of Bmp signalling.

Key words: Mouse, Limb, Anteroposterior patterning, Dorsoventral specification, Bmp signalling, Homologous recombination

Introduction

The vertebrate limb is a model of choice with which to address fundamental questions related to signal transduction and pattern formation. Through the combination of experimental embryology and molecular genetics, the mechanisms that control growth and patterning of the limb along its three axes are beginning to be understood (reviewed by Niswander, 2003; Tickle, 2003).

Proximodistal (PD) development depends on the apical ectodermal ridge (AER), a transient epithelial structure rimming the distal margin of the limb bud (Saunders, 1948; Summerbell, 1974) that provides molecular signals to sustain cell proliferation in the underlying mesenchyme. *Fgf8* and *Fgf4* (and to a lesser extent *Fgf9* and *Fgf17*) are expressed in the AER and promote normal limb development by maintaining the expression of another Fgf family member, *Fgf10*, in the mesenchyme (Sun et al., 2002). Reciprocally, in *Fgf10*$^{-/-}$ mutant embryos, the AER does not form, leading to a complete truncation of fore- and hindlimbs (Sekine et al., 1999). Thus, it appears that PD limb outgrowth is dependent upon a positive feedback between the AER- and apical mesoderm-specific Fgf activities.

The key organizer for the anteroposterior (AP) axis has been identified as a population of cells from the posterior mesenchyme, called the zone of polarizing activity (ZPA), that specifically secretes the sonic hedgehog (Shh) protein (reviewed by Pearse and Tabin, 1998). Heterotopic grafting of the ZPA (Saunders and Gasseling, 1968) or of *Shh*-expressing cells (Riddle et al., 1993) to the anterior margin of the limb bud leads to a mirror duplication of the digits. Conversely, the *Shh* null mutation provokes a dramatic loss of the anterior skeleton of the autopod (handplate/footplate) where a single digit I remains (Chiang et al., 2001). However, although Shh is necessary for normal expansion of the AP axis, the limb field is prepatterned along the AP axis prior to *Shh* activation through mutual genetic antagonism between *Gli3* and *Hand2* (te Welscher et al., 2002).

Dorsoventral (DV) asymmetry is regulated, after limb bud formation, by the ectoderm. The dorsal and ventral limb ectoderm domains express, respectively, *Wnt7a* and *En1*. Mutations in both these genes have revealed that *En1* is necessary to repress *Wnt7a* expression in the ventral ectoderm and that Wnt7a is the key inducer of *Lmx1b* in the dorsal mesenchyme. Thus, the *En1* mutation leads to the ectopic ventral expression of *Wnt7a* in the ectoderm and *Lmx1b* in the mesoderm, and the distal structures develop with bi-dorsal characteristics (Loomis et al., 1996; Cygan et al., 1997). Conversely, in the absence of Wnt7a, the dorsal pattern of the

autopod is not established and the limb appears biventral (Parr and McMahon, 1995).

These three organizing centres do not work independently. Rather, patterning and growth of the limb in three dimensions is coordinated through complex interactions between the different limb organizing centres (reviewed by Niswander, 2002). For example, AER induction depends not only on lateral plate-produced Fgfs but also on DV ectoderm polarity. This is related to Bmp signalling which is required both for DV patterning and AER induction (Ahn et al., 2001; Pizette et al., 2001).

Msx genes encode homeodomain transcription factors and their expression is associated with epithelio-mesenchymal interactions at many sites in vertebrate embryos such as limb buds, craniofacial processes and tooth buds (Hill et al., 1989; Robert et al., 1989) (reviewed by Davidson, 1995). Knockout experiments have shown that *Msx1*-null mutations provoke defects in craniofacial development, cleft palate, inner ear malformations and tooth agenesis (Satokata and Maas, 1994; Houzelstein et al., 1997), whereas *Msx2* null mutations lead to abnormal tooth development, loss of fur and reduced and disorganized cerebellar lobules (Satokata et al., 2000) (Y.L., M-A.N., A.B. and B.R., unpublished). Single Msx homozygous mutants ($Msx1^{-/-}$ or $Msx2^{-/-}$) do not display gross limb abnormalities. However, several lines of evidence suggest that this gene family may play a crucial role in limb morphogenesis. First, both genes are prominently expressed in the limb field from the earliest stages of limb formation and, later on, in both the AER and the subjacent mesenchyme. Furthermore, they require functional interactions between ectoderm and mesoderm for their expression and have been proposed to mediate transduction of inductive signals at this site (Davidson et al., 1991; Robert et al., 1991). Second, misexpression of *Msx1* in dorsal ectoderm of the chick limb bud can induce formation of ectopic AERs, similarly to misexpression of a constitutively activated Bmp receptor, suggesting that Msx1 acts downstream of Bmp signals in AER induction (Pizette et al., 2001).

The co-expression of *Msx1* and *Msx2* and their possible overlapping functions might explain the absence of a limb phenotype in either of the simple mutants. We have analysed $Msx1^{-/-}$; $Msx2^{-/-}$ double mutant embryos. We observed that Msx genes play a role at several stages of limb development and that their mutation affects the three organizing centres. In the double mutant, dorsoventral patterning is disturbed at the anterior border of the limb bud and this precludes AER formation anteriorly. Msx genes are necessary for the regression of the AER at later stages. The mutation of the two genes leads to further malformations along the AP axis, initially by preventing the development of the anteriormost region of the autopod (distal segment) and zeugopod (intermediate segment) and, later on, by provoking the abnormal overgrowth of the remaining anterior part of the autopod mesenchyme. These defects can be explained in the context of a role for Msx genes in Bmp signal transduction.

Materials and methods

Mice and embryos

Insertional mutation of the mouse *Msx1* homeobox gene by an *nlacZ* reporter gene and genotyping of the animals have been described previously (Houzelstein et al., 1997). The null allele of *Msx2* was produced following a similar strategy (see Fig. S1 in the supplementary material). In brief, the recombination vector contained 3.1 kb and 5.6 kb of *Msx2* sequences from the 5′ and the 3′ regions of the gene, respectively. *Msx2* coding and intron sequences were replaced by an *nlacZ-neo* cassette, such that the nuclear β-galactosidase is produced from the *Msx2* initiation ATG. This construct was electroporated into 129 derived HM1 ES cells (Magin et al., 1992) (a gift from Dr D. Melton) and homologous recombination events identified. Following germline transmission, the mutation was transferred to a C57BL/6 background. Subsequently, the combined *Msx1; Msx2* mutant strain was maintained on an outbred (NMRI) background. Double heterozygous animals displayed no apparent phenotype. Double homozygous embryos were obtained by $Msx1^{+/-}$; $Msx2^{+/-}$ intercrosses. Day of the plug was considered as 0.5 dpc.

In situ hybridization

Whole-mount in situ hybridization was performed as described previously (Houzelstein et al., 1997). RNA probes were generated from the following DNA fragments: *Fgf8* was a complete cDNA sequence obtained by PCR (forward primer CGC TCG GGC TCT CAG TGC TCC; reverse primer: GAG CTG GGC GAG CGC CTA TCG). *Alx4* was a gift from F. Meijling; *Hoxd11* from P. Dollé; *Fgf4* from G. Martin; *Fgf9* from R. Kelly; *Shh* from A. McMahon; *En1* from K. Schughart; *Lmx1b* from R. Johnson; *Bmp2, Bmp4* and *Bmp7* from B. Hogan; gremlin from R. Zeller; and *Pax9* from R. Balling.

Histology, cell death analysis and skeletal preparation

Skeletal preparation was as described in Zhang et al. (Zhang et al., 1995). Histological sections were carried out as described in Kaufman (Kaufman, 1994). For whole-mount cell death detection, embryos were fixed overnight in 4% paraformaldehyde and then dehydrated in methanol for long-term storage at –20°C. TUNEL analysis was performed on rehydrated embryos using the ApopTag Peroxidase detection kit (Q.BIOgene) according to the manufacturer's protocol for tissue cryosections and cells.

Results

Skeleton phenotype at 14.5 dpc

$Msx1^{-/-}$; $Msx2^{-/-}$ double homozygous mutants display numerous deleterious defects and do not survive, on the NMRI outbred background we used, beyond the 15th day of gestation. At 14.5 dpc, the three segments of the double-null mutant limbs (i.e. from proximal to distal: stylopod, zeugopod, autopod), as well as the scapula and the pelvic girdle, were present but shortened (about 3/4 of the normal size) (Fig. 1A,B). In the autopod of control embryos two phalanges were visible at this stage, whereas, in the double-null mutants, only one had developed. In addition the interdigital webbing was retained (Fig. 1C-F).

Abnormalities along the anteroposterior axis were also very severe. They were confined to the anterior elements of the skeleton and displayed apparently paradoxical features. The main feature was a general truncation of the anterior part of the limbs with an almost systematic loss of the anterior element of the zeugopod and a frequent oligodactyly (Fig. 1A,B) (Table 1). In oligodactylous animals, the missing digit was always the anteriormost one (digit I). Carpals and tarsals were also affected in the anterior region. The posterior elements were present, the medium elements severely reduced or barely visible, and the anteriormost ones absent (Fig. 1C,D). Connections were maintained with the remaining digits, which

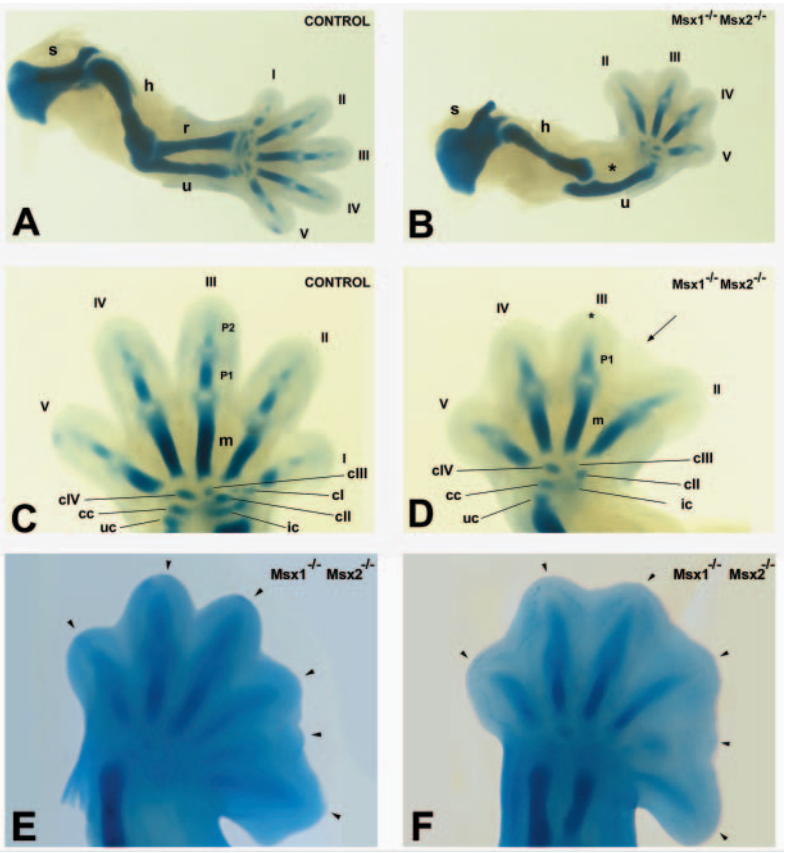

Fig. 1. Limb phenotype of *Msx1*$^{-/-}$; *Msx2*$^{-/-}$ double-null embryos at 14.5 dpc. (A-F) Alcian blue-stained skeletal preparations. (A,B) Forelimb of a control (A) and a double homozygous (B) embryo. There is an overall reduction in size of the limb in the mutant and the radius is absent (asterisk). (C,D) Higher magnification of the autopods of the embryos shown in A and B, respectively. Only one phalange has developed on digits II to V in the double mutant (asterisk) and the interdigital webbing has not regressed. The arrow indicates the presence of an abnormal distal mesenchyme condensation between digit II and III. The metacarpal (m), the first (p1) and second (p2) phalanges are indicated only for digit III, with the missing phalange indicated by an asterisk for the double mutant. (E,F) Autopods of two polydactyl double mutant embryos. In both cases, six digit formations are present (arrowheads) and the anterior-most digit is longer than a normal thumb. (E) The radius is completely absent whereas it is almost normal in F. CI-IV, carpal I to IV; cc, central carpal; h, humerus; ic, intermedioradial carpal; r, radius; s, scapula; u, ulna; uc, ulnar carpal. (C-F) Anterior is towards the right.

allowed confirmation of their identity. In addition, double-null embryos lacked the pubis bone (data not shown), which corresponds to the anterior part of the pelvis, based on phylogenetic and embryological considerations (Hinchliffe and Johnson, 1980; Knezevic et al., 1997).

However, almost one quarter of the double-null forelimbs (4/18) and two out of 12 hindlimbs presented with five digits (Table 1). Furthermore, two forelimbs with six digits were observed (Fig. 1E,F; Table 1). In these examples, the anteriormost digit was longer than a normal thumb whereas the digit placed just posterior to it was reduced in length, suggesting that the most anterior digit had a more posterior identity. The complex double-null phenotype thus varied from an oligodactylous to a polydactylous morphology.

AER maturation but not initiation is affected in double-null mutants

The size of double-null limb buds was reduced by about one third compared with controls at 10.5 to 11.5 dpc, even in somite-matched embryos (compare, for example, Fig. 3E with 3F, Fig. 3G with 3H or Fig. 4G with 4H). This prompted us to investigate the activity of the AER. *Fgf8* is expressed specifically in pre-AER and AER cells (Loomis et al., 1998). *Fgf8* expression was detected as early as the 14-somite stage in the double-null embryo limb field, indicating that AER initiation took place at the normal stage (Fig. 2A,B). However, its subsequent maturation was impaired. During mouse limb development, the cells giving rise to the AER are recruited from the ventral part of the limb bud ectoderm to form a broad pre-AER domain that becomes progressively thinner and ends as a thin strip of cells at the tip of the bud (Loomis et al., 1998). In double-null embryos, at 10.5 and 11.5 dpc, the AER appeared shorter and more diffuse than normal (Fig. 2C-H) as shown by *Fgf8* (Fig. 2C,D) or *Bmp7* (Fig. 2E,F) expression profiles, and histological analysis (Fig. 2 G,H). In addition, *Fgf4* (Fig. 2I,J) and *Fgf9* (data not shown), two other Fgf genes normally expressed in the AER as early as 10.5 dpc, were barely detectable at this stage in double-null embryos, proving that the activity of the AER was also delayed.

The anteriormost part of the double-null mutant limb regresses before the twelfth day of development

At 11.5 dpc, a sharp discontinuity was visible at the anterior of the limbs that appeared truncated anteriorly (Fig. 3A,B; see also Fig. 7C,D). At this stage, *Fgf8* is normally expressed over the entire AER, while *Fgf4* expression is absent from its anterior third (Niswander and Martin, 1992; Crossley and Martin, 1995) (see also Fig. 6A). These markers were analysed together in double in situ hybridisation. At 11.5 dpc, *Fgf4* was expressed at a normal level in double-null limb buds but its expression pattern was abnormal relative to that of *Fgf8*. As expected, the AER of control embryos displayed an anterior domain expressing *Fgf8* (Fig. 3A, red staining) but devoid of

Table 1. Quantitation of defects affecting limbs in *Msx1*$^{-/-}$; *Msx2*$^{-/-}$ double mutant

Phenotype		Forelimb	Hindlimb
Radius or tibia	Missing	14/18	17/18
	Truncated	3/18	1/18
	Normal	1/18	0/18
Number of digits	3	2/18	7/18
	4	10/18	9/18
	5	4/18	2/18
	6	2/18*	0/18

*One associated with a normal radius, one with a truncated radius.

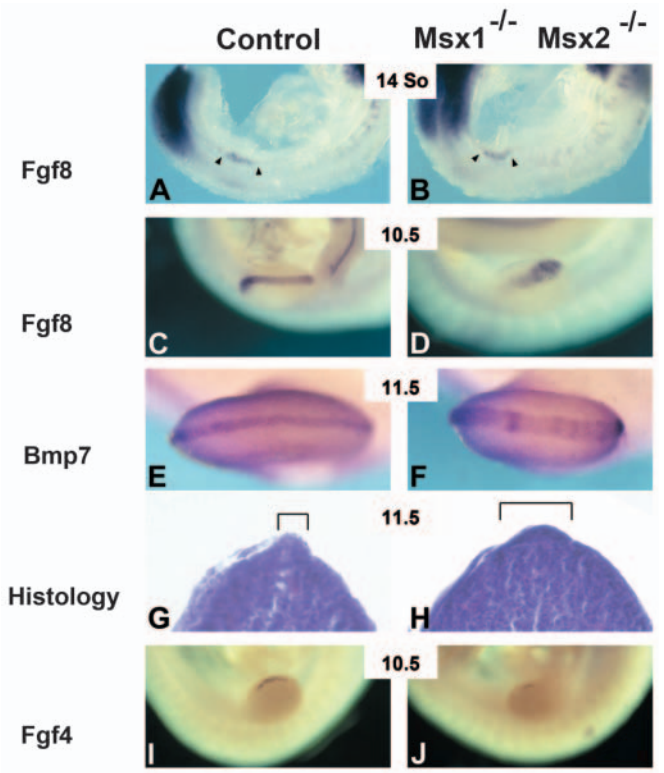

Fig. 2. AER maturation, but not initiation, is impaired in *Msx1*$^{-/-}$; *Msx2*$^{-/-}$ double-null embryos. (A,B) Initiation of the AER is not delayed in the double mutants as revealed by *Fgf8* expression at the 14-somite stage. In both panels, arrowheads delimitate the forelimb territory. (C,D) At 10.5 dpc, the AER in the double-null embryo appears shorter and thicker than in the control. (E-H) At 11.5 dpc, the AER remains thicker than normal as revealed by *Bmp7* expression (E,F) or histological analysis of transverse sections (G,H). (I,J) The level of *Fgf4* expression in the AER at 10.5 dpc is lower in the double mutants. All panels display forelimbs and anterior is towards the right in A-F,I,J.

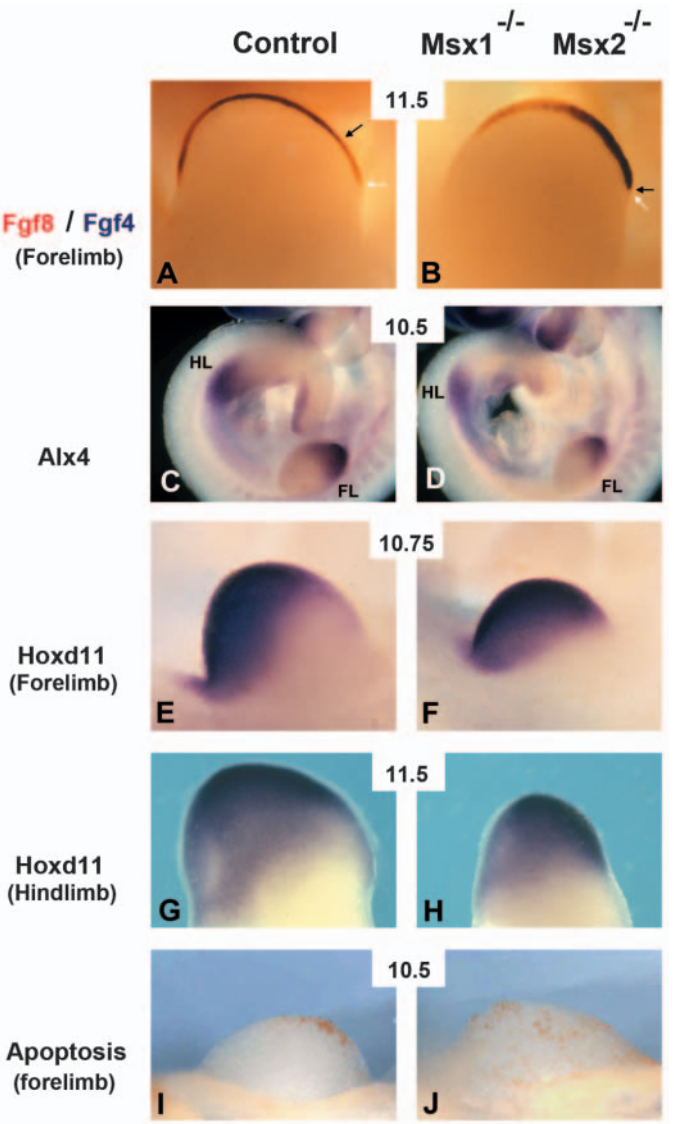

Fig. 3. The anteriormost part of the limb buds fails to develop in *Msx1*$^{-/-}$; *Msx2*$^{-/-}$ double mutant embryos. (A,B) Double in situ hybridisation with *Fgf8* (red) and *Fgf4* (purple) probes on control (A) and *Msx1*$^{-/-}$; *Msx2*$^{-/-}$ double mutant (B) embryos. At 11.5 dpc, in control embryos, the AER displays an anterior domain expressing *Fgf8* (red staining) but not *Fgf4* (purple staining), whereas in the double mutant the anterior expression limit is the same for both genes. Note the sharper aspect of the anterior border of the limb bud in the double mutant. White arrows indicate the anterior limit of *Fgf8* and black arrows indicate the anterior limit of *Fgf4* expression domains. (C,D) Left-side view of 10.5 dpc embryos showing both forelimbs (FL) and hindlimbs (HL). The *Alx4* expression domain, corresponding to the anterior third of the limb bud mesenchyme, is normal at this stage in the double mutant. (E,F) At 10.75 dpc, the anterior *Hoxd11*-negative domain, corresponding to the anterior third of the normal limb bud (E), is virtually absent in the mutant (F), whereas the posterior *Hoxd11*-expression domain has globally the same size as in the control. (G,H) Analysis of *Hoxd11* expression at 11.5 dpc confirms that the anterior domain is missing from the limb buds of double mutants. (I,J) Whole-mount analysis of apoptosis in limb buds at 10.5 dpc (ventral view). TUNEL staining shows no increase of apoptosis in the AER of the double mutant at E10.5. (A,B,E,F,I,J) Forelimbs. (G,H) Hindlimbs. Anterior is towards the right in all panels.

Fgf4-specific signal (Fig. 3A, purple staining). In double-null mutant embryos, *Fgf8* and *Fgf4* expression domains abutted exactly to the same anterior limit in the AER, which corresponded to the anterior limit of the ridge and to the sharp angular anterior border of the misshaped limb buds (Fig. 3B). These observations suggested that the anterior third of the AER was missing at this stage. In addition, the *Fgf4* expression domain was shifted anteriorly (Fig. 3B; see also Fig. 6B).

Cell death was unlikely to be the primary cause of AER anterior truncation. At 10.5 dpc, cell death was high in the anterior part of the AER and adjacent ventral ectoderm in control embryos, whereas, in the mutants, it was reduced and scattered over the whole ventral limb bud ectoderm (Fig. 3I,J).

The mesenchymal anterior domain was not maintained either. At 9.5 and 10.5 dpc, *Alx4* is specifically expressed in the anterior third of the limb bud mesenchyme. Taking into account the smaller size of the double mutant limb buds, the *Alx4* expression pattern appeared similar in double-null and normal embryos at both 9.5 (data not shown) and 10.5 dpc (Fig. 3C,D). Therefore, until 10.5 dpc the anterior mesenchyme of the double mutant limb bud was present and apparently correctly specified. At 11.5 dpc, *Alx4* is completely switched

off in the autopod. We thus relied on *Hoxd11* expression, which is symmetrical at 10.5 dpc in the distal part of the limb mesenchyme but becomes progressively polarized along the anteroposterior axis and is totally excluded from the anteriormost, future digit I (thumb) region from 11.5 dpc onwards (Charité et al., 2000; Chiang et al., 2001). At 10.5 dpc, no difference was observed between control and double mutant embryos (data not shown). However, 6-8 hours later (10.75 dpc, 37-39 somites), when *Hoxd11* expression begins to be excluded from the future digit I region, we observed a poor polarization of this domain in the double-null mutants. The size of the *Hoxd11* expression domain was approximately the same in double-null and control embryos, but the *Hoxd11* negative domain was almost absent in the mutant whereas it represents normally about one third of the limb volume at this stage (Fig. 3E,F). At 11.5 dpc, in double-null embryos, we observed a complete absence of the *Hoxd11* expression-free anterior region (Fig. 3G,H). Loss of mesenchyme with an anterior identity was confirmed using markers such as *Hoxd12*, which is expressed similarly to *Hoxd11* (data not shown) and *Bmp4* (Fig. 7C,D).

These results, together with the morphological aspect of the double-null limb buds, demonstrate that the region corresponding to the anteriormost digit disappears between 10.5 and 11.5 dpc.

The dorsoventral polarity of the limb bud is altered anteriorly in double-null mutant embryos, precluding AER formation in this region

To analyse the possible involvement of Msx genes in DV polarity, we resorted to two markers of limb DV asymmetry. The first one, *En1*, is specifically expressed in the ventral ectoderm and the ventral AER of the limb bud, as early as 9.5 dpc (Loomis et al., 1998). At 9.75 dpc (24 somites) (Fig. 4A,B) and 10.5 dpc (data not shown), *En1* expression was reduced in double-null limbs. However, at 11.5 dpc, *En1* signal was detected similarly in control and double-null embryos, with the exception of the anterior part of the AER, which is missing at this stage in the double mutant (Fig. 4C,D). The second one, *Lmx1b*, is a specific marker of the dorsal mesenchyme and a read-out of ectodermal Wnt7a activity (Riddle et al., 1995; Cygan et al., 1997). At 9.5 dpc, no obvious abnorma1ity in *Lmx1b* expression could be detected (data not shown) but, as early as 10.5 dpc, an ectopic ventral expression domain was visible at the anterior aspect of the double-null limb bud (Fig. 4E,F). This result was confirmed at 11.5 dpc. At this stage, the anterior ectopic expression domain corresponded precisely to the part of the limb that is devoid of AER (Fig. 4G-I). Thus, anteriorly, the normal DV boundary is not established in the double-null embryo limb bud. Considering the relationship between DV boundary formation and AER induction (Zeller and Duboule, 1997; Pizette et al., 2001), this is the most likely explanation for the absence of AER anteriorly. As the AER is required to maintain the underlying mesenchyme (Dudley et al., 2002), this would lead, at later stages, to the loss of anterior mesenchyme and truncation of the anterior skeleton elements.

AER regression is impaired in double-null mutant

Regression of the AER is retarded in double-null embryos. At 12.5 dpc, the AER of control embryos, as revealed by the expression of *Fgf8*, was present only at the tips of the digit

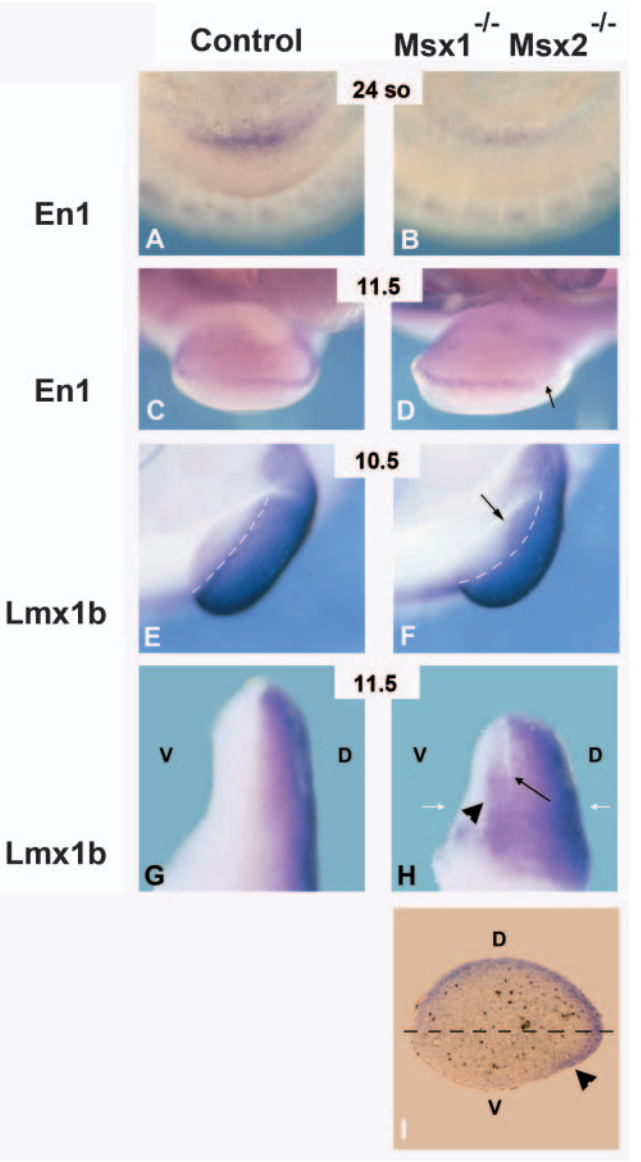

Fig. 4. Dorsoventral specification is altered in the double-null limb buds. (A-D) *En1* expression in control (A,C) and double-null mutants (B,D): limb buds are viewed from their distal tip with their ventral side facing upwards. Anterior is towards the right. *En1* expression level is reduced in the limb field at 9.5 dpc (24 somites) (A,B) and is undetectable anteriorly at 11.5 dpc (C,D) in the double mutant (D, arrow). (E-I) *Lmx1b* expression in control (E,G) and double mutant (F,H,I) embryos. (E,F) Limb buds are viewed from their distal tip with the ventral side facing towards the upper leftward side. Anterior is uppermost. The broken line indicates the normal dorsoventral boundary of the limb bud. At 10.5 dpc, the *Lmx1b* expression domain extends ventrally at the anterior aspect of the limb bud in the double mutant (arrow). (G,H) Views of the anterior border of limb buds at 11.5 dpc showing the sharp expression limit of *Lmx1b* at the level of the AER in the control (G), whereas the *Lmx1b* expression domain extends ventrally in the double mutant (arrowhead) (H). The black arrow indicates the anterior limit of the AER. (I) A section of the limb bud shown in H, according to the plane indicated by the white arrows, that confirms the presence of an ectopic *Lmx1b* expression domain in the ventral mesenchyme (arrowhead). The broken line indicates the dorsoventral boundary. Dorsoventral orientation is indicated by D and V.

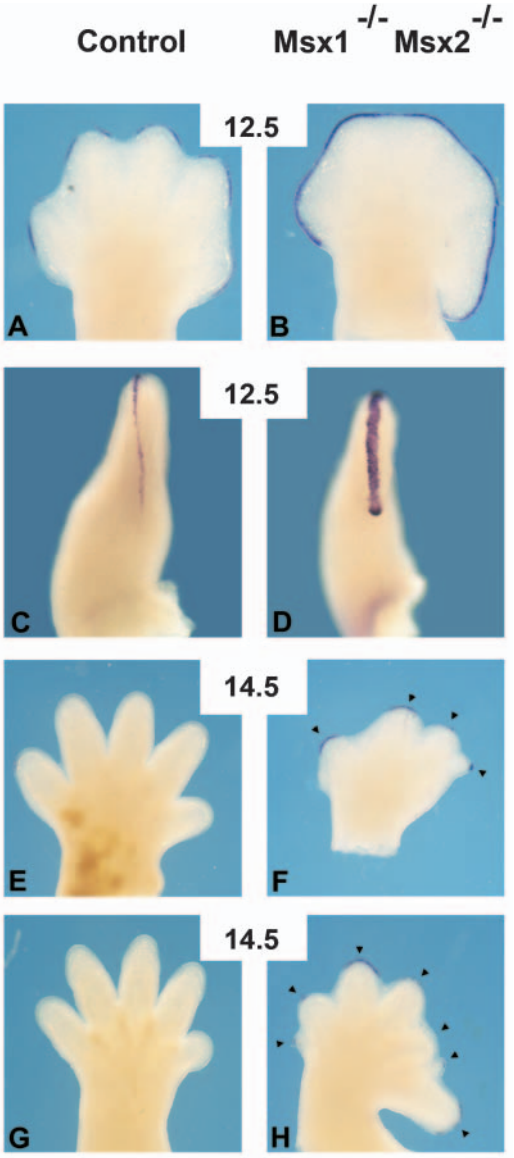

Fig. 5. AER regression is delayed in *Msx1*$^{-/-}$; *Msx2*$^{-/-}$ double mutant embryos. Comparison of *Fgf8* expression in control (A,C,E,G) and double mutant (B,D,F,H) embryos. (A-D) At 12.5 dpc, the AER has disappeared at the level of the interdigital spaces in control embryos (A). In double-null embryos, it still appears continuous (B) and thicker than normal (C,D). (E-H) At 14.5 dpc, the AER is normally absent (E,G) but still observed at the digit tips of double-null embryos (F,H, arrowheads). At this stage, the *Fgf8* expression pattern confirms the variability of the limb phenotypes ranging from oligodactyly (F) to polydactyly (H). (A-D,G,H) Forelimbs. (E,F) Hindlimbs. (C,D) Anterior views of A,B, respectively. Anterior is towards the right in A,B,E-H.

anlagen and had disappeared at the level of the interdigital webbing (Fig. 5A). By contrast, in the double-null mutants, the AER was still continuous along the whole apex of the limb (Fig. 5B) and appeared thicker than normal (Fig. 5C,D). At 14.5 dpc, *Fgf8* expression was still detectable at the tip of the digits in double-null embryos (Fig. 5E,F). *Fgf8* overexpression was often correlated with the presence of supernumerary digit primordium tips, especially in forelimb buds where up to seven digit tips were observed (Fig. 5H).

In conclusion, Msx genes act in two different ways on AER formation. In a first period (9.5 to 11.5 dpc), the *Msx1*; *Msx2* double mutation leads to AER truncation and incomplete maturation but, later on (12.5 to 14.5 dpc), it provokes its persistence beyond the normal stage.

A later effect on anteroposterior polarity in double-null mutant limbs

In addition to AER persistence, overgrowth of the anterior-distal mesenchyme of the handplate was observed from 11.75 dpc in a large proportion of double-null mutant limbs, which may underlie the polydactyly observed at later stages (compare, for example, Fig. 5G with 5H, Fig. 6C with 6D, Fig. 6G with 6H or Fig. 7G with 7H). This was mainly observed in the forelimb whereas the hindlimb generally displayed only a discrete anterior deformation (compare Fig 5E with 5F or Fig. 6E with 6F). In addition, the extent of the outgrowth was variable from one individual to another and sometimes from one side to the other in the same embryo.

The first sign of this abnormal limb polarisation was indicated by *Fgf4* expression. In the normal mouse at 11.5 dpc, *Fgf4* expression is observed in the apicoposterior part of the AER, but excluded from the ridge overlying the *Shh*-expressing mesenchymal domain (Lewandoski et al., 2000). In the double-null mutant, the *Fgf4* domain was slightly shifted anteriorly, correlatively with the loss of the anterior part of the AER and the anterior extension of *the Shh* expression domain (Fig. 6A,B,I,J). By 11.75 dpc, the remaining part of the AER of the double-null mutant appeared to extend anteriorly (data not shown). The expression of *Fgf4,* which normally disappears at this stage, persisted anteriorly in the double-null mutant AER and was still detectable at its anterior tip up to 12.5 dpc, whereas in control embryos, *Fgf4* expression had been switched off for more than 12 hours. This persistent expression domain corresponded to the tip of the anterior deformation observed at this stage (Fig. 6C,D).

Correlatively, overgrowth of the mesenchyme was observed, mainly in forelimbs. As the anterior outgrowth appeared secondarily on truncated limb buds devoid of anterior mesenchyme, we investigated the identity of outgrowing cells using the *Hoxd11* marker. At 12.5 dpc, similar to 11.5 dpc, a prominent expression was observed in the anterior outgrowth of the limb in double-null embryos (Fig. 6F,H). Therefore, the whole limb bud mesenchyme of the double mutants assumes a posterior identity. Our interpretation is that the anterior region, being devoid of AER, does not grow out and even regresses. Secondarily, persistent *Fgf4* activity at the anterior end of the AER together with *Fgf8* activity may lead to the overgrowth of the remaining anterior mesenchyme, resulting in the anomalous shape of the limb observed from 12.5 dpc onwards. Proliferation rate was not noticeably enhanced, as judged by expression of phosphorylated histone H3 or cyclin D1 (data not shown). However, at this stage, all limb bud cells are actively dividing, and a slight increase in the proliferation rate anteriorly would not be detected by these methods.

In the limb, posterior identity is associated with the expression of *Shh*, such that its anterior misexpression leads to pre-axial polydactyly (reviewed by Hill et al., 2003). In the double-null, *Shh* was weakly expressed at 10.5 dpc (data not

shown) but its expression level was similar to control at 11.5 dpc (Fig. 6I,J). At this stage, in accordance with the normal expression of other mesenchymal markers posteriorly, the domain of *Shh* expression was normal in most cases, with the exception of a slight anterior extension (Fig. 6I,J). However, in some embryos, a small anterior ectopic domain of *Shh* expression could be observed, exclusively in the forelimbs (four forelimbs out of 14 recovered at 11.5 dpc) (Fig. 6J). The extent of the anterior outgrowth at 12.5 dpc may correlate with the intensity of *Shh* ectopic expression at earlier stages, but no direct evidence can be provided at present to support this hypothesis. In hindlimbs, *Shh* expression appeared as a single posterior domain but slightly displaced distally (not shown).

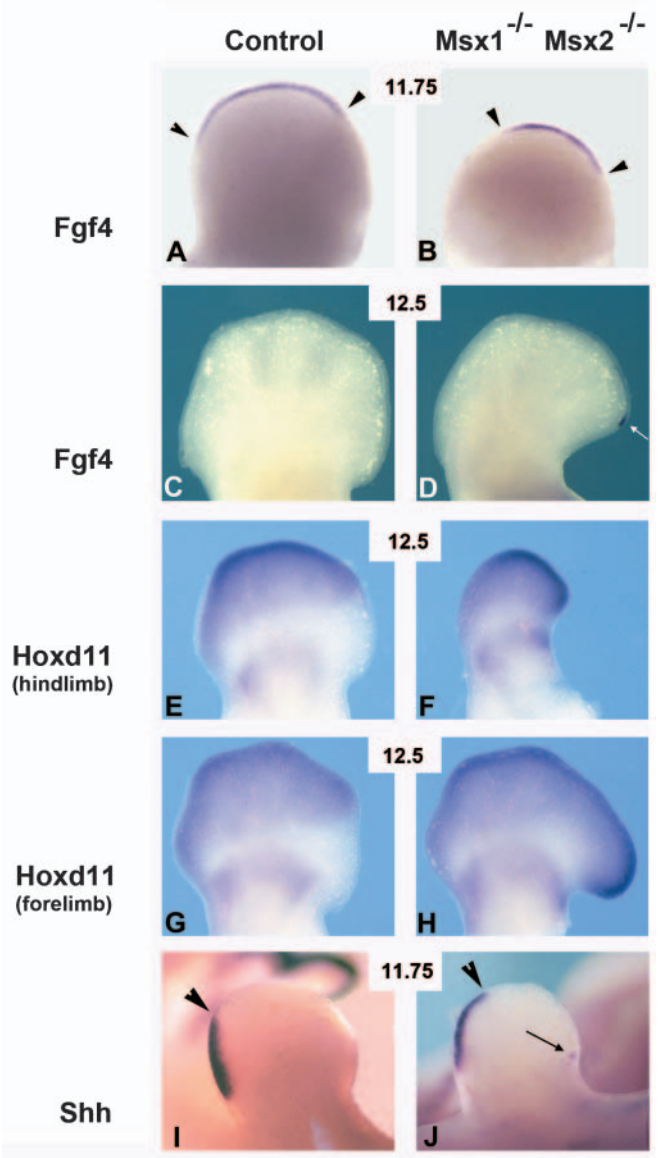

Fig. 6. Anteroposterior polarisation of the limb buds is affected in *Msx1*$^{-/-}$; *Msx2*$^{-/-}$ double mutant embryos after 11.5 dpc. (A,B) At 11.5 dpc, in normal embryos, *Fgf4* is expressed in the posterodistal part of the AER, and excluded from the anterior fourth of the AER. In the double mutants, *Fgf4* expression level is normal but expression domain is shifted anteriorly (A,B, arrowheads). (C,D) At 12.5 dpc, *Fgf4* is still detectable at the anterior tip (white arrow in D) of the AER in double mutant embryos. (E-H) *Hoxd11* is expressed only in the region corresponding to the future digits II to V in both normal hind- (E) and forelimbs (G). In the double mutants (F,H), it is expressed along the whole distal mesenchyme regardless of whether the limb bud (generally hindlimbs) is truncated (F) or, conversely (essentially forelimbs), overgrown anteriorly (H). (I,J) In a few double mutant embryos, *Shh* is faintly expressed ectopically at the anterior margin of the forelimbs (J, arrow). The posterior domain is slightly shifted distally (arrowheads). (A-D,G-J) Forelimbs. (E,F) Hindlimbs. In all panels, anterior is towards the right.

Bmp signalling

Many of the double-null limb defects are reminiscent of phenotypes observed when Bmp signalling is experimentally reduced during limb development (see Discussion). *Bmp4* has been shown to interact genetically with *Msx1* in complex and reciprocal induction processes (Chen et al., 1996). In the limb, Msx genes have been proposed to be downstream targets of the Bmp signal in AER induction (Pizette et al., 2001). In double-null embryos, *Bmp4* was not downregulated at early stages of limb development. At 9.5 dpc, when expression of *Bmp4* is confined to the ventral ectoderm, its expression domain appeared normal (data not shown). At 10.5 dpc (32-35 somites) (Fig. 7A) and 10.75 dpc (37-40 somites) (data not shown), *Bmp4* is expressed strongly in the AER and at a lower level in the mesenchyme where its expression is restricted to the posterior (strong expression) and the anterior (weaker expression) aspects of the limb bud. At these stages, expression of *Bmp4* was not significantly altered in the mesenchyme or in the remnant of the AER in the double-null mutant (Fig. 7B and data not shown). At 11.5 dpc, the posterior *Bmp4* expression domain was still present in the mesenchyme and the truncated AER also expressed this gene at a normal level. The anterior *Bmp4* expression domain was missing, in conformity with the general loss of mesoderm of anterior identity at this stage (Fig. 7C,D). Thus, up to 11.5 dpc, the analysis of *Bmp4* expression confirmed the agenesis of the limb anterior domain in double-null embryos but did not reveal any obvious downregulation of this gene in more posterior regions.

At 12.5 dpc, *Bmp4* expression, in the mesenchyme, is mainly concentrated in the interdigital spaces and digit anlagen. In the mutant, the *Bmp4* transcript level was not altered, with the exception of a slight decrease in the interdigital webbing (data not shown). At 13.5 dpc, *Bmp4* expression was present in the digit anlagen of both controls and mutants (Fig. 7E,F). It was also observed in the distal mesenchyme of control embryos (Fig. 7E, arrowhead), but not in the mutant (Fig. 7F), suggesting that Msx genes act upstream of Bmp4 at this site. In addition, expression was observed in the AER that remained in the double-null mutant (Fig. 7F).

Bmp2, contrary to *Bmp4*, is not normally expressed in the anterior part of the autopod. Similarly, *Bmp7* is not expressed anteriorly from 13.5 dpc. In the double-null mutant, at 13.5 dpc, the two genes were also expressed in the anterior domain, in keeping with its posterior identity. Outside this domain, expression pattern was similar but more intense in the mutant when compared with control embryos (Fig. 7G-J).

Gremlin expression was not significantly modified in the double mutant, except that it persisted somewhat longer in the interdigital spaces. Thus, gremlin expression was undetectable at 13.5 dpc in both the fore and hindlimbs of control embryos (Fig. 7K and data not shown) but was still detectable, at a low

level, in the interdigital spaces of the sole hindlimbs of the mutants (Fig. 7L and data not shown).

In conclusion, Bmp expression was not significantly modified by the Msx gene mutation. In the mutant, phosphorylation of the Smad1, 5 and 8 proteins could be detected at 10.5, 12.5 and 13.5 dpc, wherever one of the Bmp genes is expressed (data not shown), indicating that Msx proteins do not interfere with the first steps of Bmp signalling.

Discussion

Loss of Msx function does not preclude limb development, but elicits several patterning defects

We report the phenotype of limb buds in the *Msx1*$^{-/-}$; *Msx2*$^{-/-}$ double mutant. Three Msx genes have been identified in the mouse genome. Only *Msx1* and *Msx2* are expressed in the limb, while *Msx3* is expressed exclusively in the neural tube (Shimeld et al., 1996; Wang et al., 1996) (reviewed by Bendall and Abate-Shen, 2000). We further verified that *Msx3* is not upregulated in the limbs of double mutants (data not shown). Therefore, the *Msx1*$^{-/-}$; *Msx2*$^{-/-}$ double mutant does not produce any functional Msx protein in the limb. Expression of both genes is prominent in the limb bud, in both the AER and the distal mesenchyme which is under the influence of the AER (Robert et al., 1989; Coelho et al., 1991a; Robert et al., 1991). Although the mechanism of mesodermal cell specification at this site is still controversial (Dudley et al., 2002), the interaction between ectoderm and mesoderm is crucial for limb outgrowth and patterning (Saunders, 1948; Summerbell, 1974; Rowe et al., 1982). Msx gene expression in the limb bud requires functional ectoderm-mesoderm interactions, and it has been proposed that these genes may play a crucial role in limb patterning (Davidson et al., 1991; Robert et al., 1991). In spite of this, limb buds do form in the *Msx1*$^{-/-}$; *Msx2*$^{-/-}$ double mutants. All three segments (stylopod, zeugopod, autopod) are present, as well as the scapula/pelvis, and they are only moderately reduced in size along the proximodistal axis. Skeletal elements are nevertheless severely affected. The anterior bone of the zeugopod (radius, tibia) is nearly always truncated and in many cases, missing in the double mutant. Carpal and tarsal bones are also missing anteriorly, and anterior preaxial oligodactyly is frequent. Anterior limb truncation is thus the most constant phenotype observed. However, at the level of the autopod, this truncation is often compensated by a secondary outgrowth of the handplate that extends anteriorly and may lead to polydactyly. Thus, two phases can be distinguished in the function of Msx genes in the limb: an early one (before 11.5 dpc), when the genes are required to specify the anterior limb region; a later one (after 11.5 dpc), when they contribute to restrict the activity of the AER and allow completion of limb patterning.

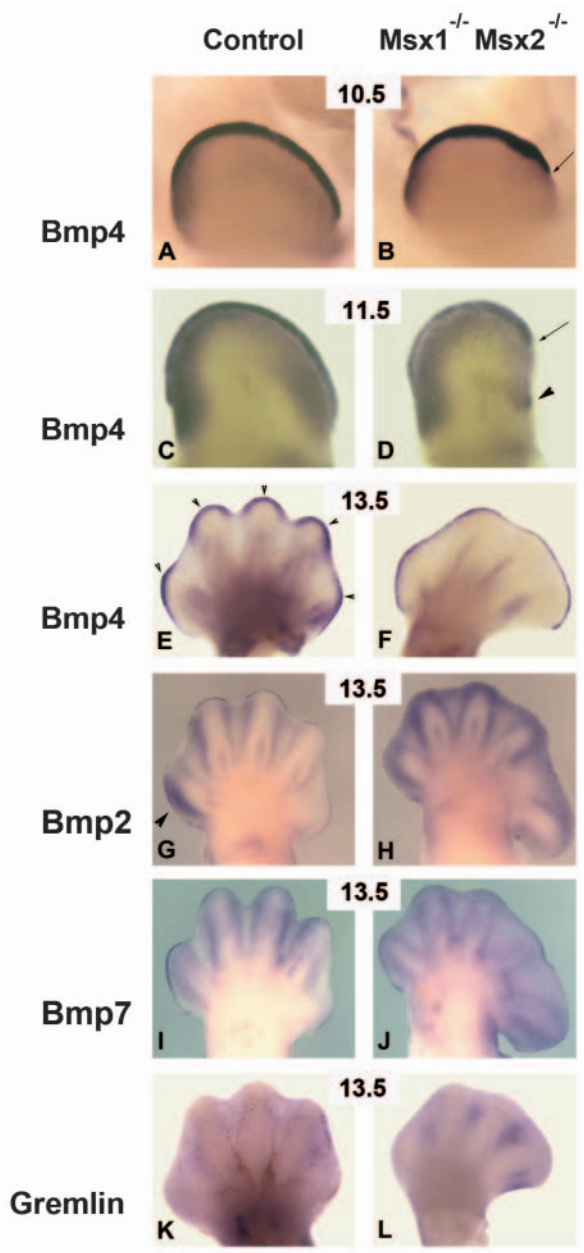

Impairment of Bmp signalling may explain many aspects of the phenotype

Relationships between Bmp and Msx proteins have been extensively documented. Msx genes are downstream targets of

Fig. 7. Bmp signalling in double mutant limbs. (A) At 10.5 dpc, in control embryos, *Bmp4* is expressed in the AER, in the posterior mesenchyme and in a faint anterior domain of the limb bud. (B) *Bmp4* expression is similar in the double-null limb bud. The anterior limit of the *Bmp4* expression domain in the ectoderm corresponds to the anterior limit of the AER (black arrow). (C,D) At 11.5, owing to the anterior truncation of both the AER (arrow) and mesenchyme, the anterior *Bmp4* expression domain is almost completely absent in the mutant. A reduced *Bmp4* expressing domain is still present at the proximal anterior border (arrowhead). In the rest of the limb bud, *Bmp4* expression is normal. (E,F) At 13.5 dpc, *Bmp4* expression is observed in the finger tip mesenchyme of control embryos (E, arrowheads) but not in the mutants (F). By contrast, expression is observed in the remaining AER of the double-null mutants (F) which has regressed at this stage in control embryos. (G,H) At 13.5 dpc, *Bmp2* expression is similar in the control and the double mutants, except that no negative anterior domain is observed. In the control (G), the arrowhead indicates a posterior domain of the limb bud that expresses *Bmp2* at a higher level. (I,J) *Bmp7* is expressed similarly to *Bmp2* in control and mutant limbs. (K,L) Gremlin expression persists slightly longer in the interdigital webbing of the mutants. The dark proximal domain in K is an artefact due to the thickness of the specimen at this site. (A-J) Forelimb buds, (K,L) hindlimb buds. In all panels, anterior is towards the right.

Bmp proteins at many sites in the embryo (reviewed by Davidson, 1995; Bendall and Abate-Shen, 2000). As such, they may be required for Bmp signal transduction. Reciprocally, they can act upstream of Bmp genes and are required in some cases for their expression. This double role is best exemplified in the tooth germ where ectodermal Bmp4 induces *Msx1* expression in the underlying mesenchyme (Vainio et al., 1993). Subsequently, Msx1 is necessary for mesenchymal *Bmp4* expression, as shown by the downregulation of this gene in the tooth germ mesenchyme of the *Msx1*$^{-/-}$ mutant (Chen et al., 1996; Zhang et al., 2000). In the palatal mesenchyme, Msx1 is required for expression of both *Bmp2* and *Bmp4*, and a *Bmp4*-expressing transgene rescues the cleft-palate lethal phenotype of *Msx1*$^{-/-}$ homozygous mutants (Zhang et al., 2002).

In the limb, a number of data have shown that Msx genes are downstream targets of Bmp signalling. At early stages, *Msx1* and *Msx2* are expressed in nearly identical patterns that overlap significantly with Bmp genes, namely *Bmp2*, *Bmp4* and *Bmp7* (Ahn et al., 2001; Pizette et al., 2001). Enhanced Bmp signalling, which is observed in animals heterozygous for the Fused toes (*Ft*) mutation (Heymer and Rüther, 1999), or in mutants homozygous for a null allele of gremlin, a potent Bmp antagonist (Khokha et al., 2003), leads to an upregulation of both *Msx1* and *Msx2* expression. Reciprocally, blocking Bmp signalling in the limb ectoderm provokes a decrease of *Msx2* expression (Wang et al., 2004). Our data show that, during all phases of limb development, the absence of Msx activity leads to phenotypes that in many respects mimic the absence or decrease in Bmp signalling: delay in both maturation and regression of the AER (Pizette and Niswander, 1999; Wang et al., 2004); anterior upregulation of *Fgf4* expression in the AER (Zùniga et al., 1999); tendency to anterior polydactyly (Hofmann et al., 1996; Dunn et al., 1997; Katagiri et al., 1998); and absence of interdigital tissue regression (Guha et al., 2002; Wang et al., 2004). The absence of DV specification anteriorly and the loss of the corresponding part of the AER reproduce locally the effect of Bmp-receptor inhibition (Ahn et al., 2001; Pizette et al., 2001). In limb development, Msx genes seem to act downstream of Bmp signalling, since Bmp expression profiles are little affected in the double mutant, as is the case for Smads.

AER maturation but not initiation is affected in *Msx1*$^{-/-}$; *Msx2*$^{-/-}$ double mutants

The AER is established at the boundary between dorsal and ventral ectoderm (Altabef et al., 1997; Michaud et al., 1997; Tanaka et al., 1998; Kimmel et al., 2000). At the molecular level, this boundary takes place between *Bmp*-expressing (ventrally) and non-expressing (dorsally) domains at the stage when limb buds form. In the chick, Pizette et al. (Pizette et al., 2001) have demonstrated that depletion of the ventral Bmp signal prevents *En1* expression in the ventral ectoderm and precludes AER formation. Reciprocally, activation of Bmp signalling over the whole limb ectoderm leads to induction of *En1* also in the dorsal ectoderm, which adopts a ventral identity, and abrogates AER formation. In addition, activated Bmp receptor gene expression in the dorsal ectoderm induces patches of *Fgf8* expression. Based on these and other results, these authors have proposed that Bmp signalling is governing both DV limb patterning and AER formation via the induction of *En1* and Msx genes, respectively, and that these two pathways are independent. Furthermore, they proposed that Msx genes are downstream effectors of the Bmp signal in AER formation. This is supported by two main lines of evidence: (1) *Msx1* and *Msx2* display overlapping expression patterns with *Bmp4* and *Bmp7* in ventral ectoderm at early stages of limb development; and (2) ectopic expression of *Msx1* in limb dorsal ectoderm, where Msx genes are normally not expressed at stages of AER induction, may result in the formation of ectopic ridges expressing *Fgf8*. These extra ridges would be induced by the formation of a new boundary between *Msx*-expressing and non-expressing cells. In accordance with this model, in the mouse, conditional inactivation of the *Bmpr1a* gene in limb ectoderm also elicits both DV patterning defects, involving *En1* downregulation, and the absence of AER formation (Ahn et al., 2001).

Our data confirm that Msx play an essential role in AER formation. Nevertheless, this role does not fit exactly with the model proposed by Pizette et al. (Pizette et al., 2001). First, in the absence of Msx proteins, AER is induced and maintained over the major part of the limb bud apex, implying that Msx function is required for AER formation only at the anterior margin. Second, in the anterior region where the AER does not form, this is correlated with the absence of a DV boundary, as, based on the expression patterns of *Lmx1b*, the bud is bi-dorsal in this domain. Therefore, the deficiency in AER formation does not appear to be independent of DV patterning.

In the more posterior part of the double-null limb, the AER forms, but its maturation is delayed and it remains wider than normal. This too may result from impairment in Bmp signalling. Misexpression of noggin from a transgene in the AER and over the limb ventral ectoderm, in the mouse, also leads to ventral extension of the AER (Wang et al., 2004). Our results suggest that in the absence of Msx proteins, Bmp signalling is affected along the whole apex of the limb. Anteriorly, this would result in loss of the AER, agenesis of mesoderm and lack of skeletal elements, but posteriorly only to incomplete AER maturation. Posteriorly, a deficit in Bmp signalling may be of limited effect or, conversely, other genes may fulfil the role of Msx.

During digit individualization, regression of the AER and of interdigital tissues is impaired

From 12.5 dpc to 14.5 dpc, the double-null limb phenotype is characterized by the slow and incomplete regression of the AER and the persistence of the interdigital soft tissues, preventing correct individualization of the digits. Regression of the AER is under the control of Bmp signalling. In the chick, retroviral expression of the Bmp antagonist noggin inhibits AER regression. Accordingly, from stage 24, *Msx2* is downregulated in the AER and underlying mesenchyme, whereas *Msx1* is downregulated in the posterior part of the apical mesenchyme (Pizette and Niswander, 1999). In the mouse, expression of noggin, from a transgene, in the ectoderm leads to both persistence of the AER and downregulation of *Msx2* in this structure but not in the mesenchyme, whereas *Bmp4* expression is not modified (Guha et al., 2002; Wang et al., 2004). Thus, during AER regression, Msx genes are probably under the control of Bmp signalling. Our data further suggest that they are required to transduce Bmp activity in the AER because, in the *Msx1*$^{-/-}$; *Msx2*$^{-/-}$ double-null mutants, AER regression is impaired from 12.5 dpc while *Bmp4*

expression is not modified along the apical border of the limb at this stage.

The involvement of Msx genes in interdigital tissue regression by apoptosis has been proposed by several authors (reviewed by Chen and Zhao, 1998). Both *Msx1* and *Msx2* are expressed in the interdigital tissue at the time when apoptosis takes place (Robert et al., 1989; Coelho et al., 1991b). Furthermore, this expression pattern correlates with the extent of interdigital tissue regression in different species (Gañan et al., 1998). Our results confirm this role because, in the double-null mutant, interdigital tissue webbing fails to regress. Bmp proteins have been identified as the trigger in this process (Yokouchi et al., 1996; Zou and Niswander, 1996; Macias et al., 1997; Guha et al., 2002). Whether Msx gene expression is required upstream or downstream of Bmp signalling is controversial (Ferrari et al., 1998; Merino et al., 1999). Our results suggest that, in interdigital webbing regression, Msx would act downstream of Bmp signalling as expression of Bmp2 and Bmp7 is unchanged and that of Bmp4 only slightly decreased at the stage when apoptosis is active.

Roles of Msx genes in regulating the anteroposterior polarity of the limb

Between 11.5 and 12.5 dpc, the double-null handplate, particularly in forelimbs, starts undergoing an important anterior overgrowth. This is correlated with a prominent anterior extension of the AER and persistence of *Fgf4* and *Fgf8* expression up to the anteriormost limit of the elongated AER. Experimental evidence shows that whenever the AER is elongated, or Fgf4 signalling increased, by genetic manipulation, this leads to an overgrowth of the underlying mesenchyme and later on, to anterior polydactyly (e.g. Hofmann et al., 1996; Liu et al., 2003; Wang et al., 2004). This is probably due to the mitogenic properties of Fgf proteins on limb mesenchyme (reviewed by Martin, 1998) but also to the capacity of Fgf4 to recruit cells to the limb bud from adjacent territories (Tanaka et al., 2000). Noticeably, the digits duplicated anteriorly display, in some cases, a posterior identity (Hofmann et al., 1996; Liu et al., 2003).

Anterior outgrowth, leading to polydactyly, may also be due to impairment in the transduction of Bmp signal in the absence of Msx function. Anterior polydactyly is often observed in situations where Bmp signalling is globally diminished, such as in heterozygous *Bmp4*-null mutants (Dunn et al., 1997), in *Bmp7* homozygous mutants (Luo et al., 1995; Hofmann et al., 1996) or in $Bmp4^{+/-}$; $Bmp7^{+/-}$ double heterozygous mutants (Katagiri et al., 1998). This is not necessarily associated with ectopic expression of *Shh* anteriorly (Dunn et al., 1997). Nevertheless, Bmp4 has been shown to repress *Shh* in the tooth epithelium and to act downstream of *Msx1* in this process. This property is conserved in the limb, although a role for *Msx1* at this site was not investigated (Zhang et al., 2000). We observed only a discrete and inconsistent ectopic expression of *Shh* at the anterior of mutant limb buds. However, this was observed only in the forelimb bud, which tends to produce more frequent and more extensive polydactylies than the hindlimb. In addition, the proportion of limb buds with an ectopic *Shh* domain corresponds approximately to that of polydactylous limbs at later stages. Furthermore, *Shh* upregulation may be undetectable by in situ hybridization, but nonetheless sufficiently high to induce extra digits, as exemplified by the *raz* mutant (Krebs et al., 2003). Therefore, it remains possible that Msx genes are required to repress *Shh* anteriorly, either directly or by mediating the Bmp signal.

Conversely, Msx genes may play a crucial role in the mechanisms that pattern the anterior limb region. Recent data have shown that Shh is instrumental in patterning digits V to II, and ulna/fibula in the zeugopod (reviewed by Zeller, 2004). The determinants of more anterior structures remain to be identified, and these are precisely the structures affected in the *Msx1; Msx2* double null mutant.

We are very grateful to Dr M. Buckingham for critical reading of the manuscript. We are deeply indebted to Dr Paul Barton for his support in the initiation of this project. We are indebted to Dr D. Melton for providing HM1 ES cells and to Drs R. Balling, P. Dollé, B. Hogan, R. Johnson, R. Kelly, G. Martin, A. McMahon, F. Meijling, K. Schughart and R. Zeller for providing probes. This work was supported by the Institut Pasteur, the Centre National de la Recherche Scientifique, and grants from the Association pour la Recherche contre le Cancer and the Association Française contre les Myopathies. A.B. was the recipient of fellowships from the Ministère de la Recherche and the Association pour la Recherche contre le Cancer. C.R. was funded by the European community, then by the Fondation pour la Recherche Médicale.

Supplementary material

Supplementary material for this article is available at
http://dev.biologists.org/cgi/content/full/132/13/3003/DC1

References

Ahn, K., Mishina, Y., Hanks, M. C., Behringer, R. R. and Crenshaw, E. B., III (2001). BmpR-IA signaling is required for the formation of the apical ectodermal ridge and dorso-ventral patterning of the limb. *Development* **128**, 4449-4461.

Altabef, M., Clarke, J. D. and Tickle, C. (1997). Dorso-ventral ectodermal compartments and origin of apical ectodermal ridge in developing chick limb. *Development* **124**, 4547-4556.

Bendall, A. J. and Abate-Shen, C. (2000). Roles for Msx and Dlx homeoproteins in vertebrate development. *Gene* **247**, 17-31.

Charite, J., McFadden, D. G. and Olson, E. N. (2000). The bHLH transcription factor dHAND controls Sonic hedgehog expression and establishment of the zone of polarizing activity during limb development. *Development* **127**, 2461-2470.

Chen, Y. and Zhao, X. (1998). Shaping limbs by apoptosis. *J. Exp. Zool.* **282**, 691-702.

Chen, Y., Bei, M., Woo, I., Satokata, I. and Maas, R. (1996). Msx1 controls inductive signaling in mammalian tooth morphogenesis. *Development* **122**, 3035-3044.

Chiang, C., Litingtung, Y., Harris, M. P., Simandl, B. K., Li, Y., Beachy, P. A. and Fallon, J. F. (2001). Manifestation of limb prepattern: limb development in the absence of Sonic hedgehog function. *Dev. Biol.* **236**, 421-435.

Coelho, C. N., Krabbenhoft, K. M., Upholt, W. B., Fallon, J. F. and Kosher, R. A. (1991a). Altered expression of the chicken homeobox-containing genes *GHox-7* and GHox-8 in the limb buds of limbless mutant chick embryos. *Development* **113**, 1487-1493.

Coelho, C. N., Sumoy, L., Rodgers, B. J., Davidson, D. R., Hill, R. E., Upholt, W. B. and Kosher, R. A. (1991b). Expression of the chicken homeobox-containing gene *GHox-8* during embryonic chick limb development. *Mech. Dev.* **34**, 143-154.

Crossley, P. H. and Martin, G. R. (1995). The mouse *Fgf8* gene encodes a family of polypeptides and is expressed in regions that direct outgrowth and patterning in the developing embryo. *Development* **121**, 439-451.

Cygan, J. A., Johnson, R. L. and McMahon, A. P. (1997). Novel regulatory interactions revealed by studies of murine limb pattern in Wnt-7a and En-1 mutants. *Development* **124**, 5021-5032.

Davidson, D. (1995). The function and evolution of Msx genes: pointers and paradoxes. *Trends Genet.* **11**, 405-411.

Davidson, D. R., Crawley, A., Hill, R. E. and Tickle, C. (1991). Position-dependent expression of two related homeobox genes in developing vertebrate limbs. *Nature* **352**, 429-431.

Dudley, A. T., Ros, M. A. and Tabin, C. J. (2002). A re-examination of proximodistal patterning during vertebrate limb development. *Nature* **418**, 539-544.

Dunn, N. R., Winnier, G. E., Hargett, L. K., Schrick, J. J., Fogo, A. B. and Hogan, B. L. M. (1997). Haploinsufficient phenotypes in *Bmp4* heterozygous null mice and modification by mutations in Gli3 and Alx4. *Dev. Biol.* **188**, 235-247.

Ferrari, D., Lichtler, A. C., Pan, Z. Z., Dealy, C. N., Upholt, W. B. and Kosher, R. A. (1998). Ectopic expression of Msx-2 in posterior limb bud mesoderm impairs limb morphogenesis while inducing BMP-4 expression, inhibiting cell proliferation, and promoting apoptosis. *Dev. Biol.* **197**, 12-24.

Gañan, Y., Macias, D., Basco, R. D., Merino, R. and Hurle, J. M. (1998). Morphological diversity of the avian foot is related with the pattern of Msx gene expression in the developing autopod. *Dev. Biol.* **196**, 33-41.

Guha, U., Gomes, W. A., Kobayashi, T., Pestell, R. G. and Kessler, J. A. (2002). In vivo evidence that BMP signaling is necessary for apoptosis in the mouse limb. *Dev. Biol.* **249**, 108-120.

Heymer, J. and Rüther, U. (1999). Syndactyly of Ft/+ mice correlates with an imbalance in *Bmp4* and *Fgf8* expression. *Mech. Dev.* **88**, 173-181.

Hill, R. E., Jones, P. F., Rees, A. R., Sime, C. M., Justice, M. J., Copeland, N. G., Jenkins, N. A., Graham, E. and Davidson, D. R. (1989). A new family of mouse homeobox-containing genes: molecular strucutre, chromosomal location and developmental expression of Hox-7.1. *Genes Dev.* **3**, 26-37.

Hill, R. E., Heaney, S. J., and Lettice, L. A. (2003). Sonic hedgehog: restricted expression and limb dysmorphologies. *J. Anat.* **202**, 13-20.

Hinchliffe, J. R. and Johnson, D. R. (1980). *The Development of the Vertebrate Limb: An Approach Through Experiment, Genetics and Evolution*. Oxford: Clarendon Press.

Hofmann, C., Luo, G., Balling, R. and Karsenty, G. (1996). Analysis of limb patterning in BMP-7-deficient mice. *Dev. Genet.* **19**, 43-50.

Houzelstein, D., Cohen, A., Buckingham, M. E. and Robert, B. (1997). Insertional mutation of the mouse *Msx1* homeobox gene by an *nlacZ* reporter gene. *Mech. Dev.* **65**, 123-133.

Katagiri, T., Boorla, S., Frendo, J. L., Hogan, B. L. and Karsenty, G. (1998). Skeletal abnormalities in doubly heterozygous Bmp4 and Bmp7 mice. *Dev. Genet.* **22**, 340-348.

Kaufman, M. H. (1994). *The Atlas of Mouse Development*. Academic Press. London.

Khokha, M. K., Hsu, D., Brunet, L. J., Dionne, M. S. and Harland, R. M. (2003). Gremlin is the BMP antagonist required for maintenance of Shh and Fgf during limb patterning. *Nat. Genet.* **34**, 303-307.

Kimmel, R. A., Turnbull, D. H., Blanquet, V., Wurst, W., Loomis, C. A. and Joyner, A. L. (2000). Two lineage boundaries coordinate vertebrate apical ectodermal ridge formation. *Genes Dev.* **14**, 1377-1389.

Knezevic, V., De Santo, R., Schughart, K., Huffstadt, U., Chiang, C., Mahon, K. A. and Mackem, S. (1997). *Hoxd-12* differentially affects preaxial and postaxial chondrogenic branches in the limb and regulates *Sonic hedgehog* in a positive feedback loop. *Development* **124**, 4523-4536.

Krebs, O., Schreiner, C. M., Scott, W. J., Bell, S. M., Robbins, D. J., Goetz, J. A., Alt, H., Hawes, N., Wolf, E. and Favor, J. (2003). Replicated anterior zeugopod (raz): a polydactylous mouse mutant with lowered Shh signaling in the limb bud. *Development* **130**, 6037-6047.

Lewandoski, M., Sun, X. and Martin, G. R. (2000). *Fgf8* signalling from the AER is essential for normal limb development. *Nat. Genet.* **26**, 460-463.

Liu, C., Nakamura, E., Knezevic, V., Hunter, S., Thompson, K. and Mackem, S. (2003). A role for the mesenchymal T-box gene *Brachyury* in AER formation during limb development. *Development* **130**, 1327-1337.

Loomis, C. A., Harris, E., Michaud, J., Wurst, W., Hanks, M. and Joyner, A. L. (1996). The mouse *Engrailed-1* gene and ventral limb patterning. *Nature* **382**, 360-363.

Loomis, C. A., Kimmel, R. A., Tong, C. X., Michaud, J. and Joyner, A. L. (1998). Analysis of the genetic pathway leading to formation of ectopic apical ectodermal ridges in mouse *Engrailed-1* mutant limbs. *Development* **125**, 1137-1148.

Luo, G., Hofmann, C., Bronckers, A. L., Sohocki, M., Bradley, A. and Karsenty, G. (1995). BMP-7 is an inducer of nephrogenesis, and is also required for eye development and skeletal patterning. *Genes Dev.* **9**, 2808-2820.

Macias, D., Ganan, Y., Sampath, T. K., Piedra, M. E., Ros, M. A. and Hurle, J. M. (1997). Role of BMP-2 and OP-1 (BMP-7) in programmed cell death and skeletogenesis during chicklimb development. *Development* **124**, 1109-1117.

Magin, T. M., McWhir, J. and Melton, D. W. (1992). A new mouse embryonnic stem cell line with good germ line contribution and gene targeting frequency. *Nucleic Acids Res.* **20**, 3795-3796.

Martin, G. R. (1998). The roles of FGFs in the early development of vertebrate limbs. *Genes Dev.* **12**, 1571-1586.

Merino, R., Rodriguez-Leon, J., Macias, D., Ganan, Y., Economides, A. N. and Hurle, J. M. (1999). The BMP antagonist Gremlin regulates outgrowth, chondrogenesis and programmed cell death in the developing limb. *Development* **126**, 5515-5522.

Michaud, J. L., Lapointe, F. and Le Douarin, N. M. (1997). The dorsoventral polarity of the presumptive limb is determined by signals produced by the somites and by the lateral somatopleure. *Development* **124**, 1453-1463.

Niswander, L. (2002). Interplay between the molecular signals that control vertebrate limb development. *Int. J. Dev. Biol.* **46**, 877-881.

Niswander, L. (2003). Pattern formation: old models out of the limb. *Nat. Rev. Genet*. **4**, 133-143.

Niswander, L. and Martin, G. R. (1992). *Fgf-4* expression during gastrulation, myogenesis, limb and tooth development in the mouse. *Development* **114**, 755-768.

Parr, B. A. and McMahon, A. P. (1995). Dorsalizing signal Wnt-7a required for normal polarity of D-V and A-P axes of mouse limb. *Nature* **374**, 631-640.

Pearse, R. V., 2nd and Tabin, C. J. (1998). The molecular ZPA. *J. Exp. Zool.* **282**, 677-690.

Pizette, S. and Niswander, L. (1999). BMPs negatively regulate structure and fucntion of limb apical ectodermal ridge. *Development* **126**, 883-894.

Pizette, S., Abate-Shen, C. and Niswander, L. (2001). BMP controls proximodistal outgrowth, *via* induction of the apical ectodermal ridge, and dorsoventral patterning in the vertebrate limb. *Development* **128**, 4463-4474.

Riddle, R. D., Johnson, R. L., Laufer, E. and Tabin, C. (1993). Sonic hedgehog mediates the polarizing activity of the ZPA. *Cell* **75**, 1401-1416.

Riddle, R. D., Ensini, M., Nelson, C., Tsuchida, T., Jessell, T. M. and Tabin, C. (1995). Induction of the LIM homeobox gene *Lmx1* by WNT7a establishes dorsoventral pattern in the vertebrate limb. *Cell* **83**, 631-640.

Robert, B., Sassoon, D., Jacq, B., Gehring, W. and Buckingham, M. (1989). *Hox-7*, a mouse homeobox gene with a novel pattern of expression during embryogenesis. *EMBO J.* **8**, 91-100.

Robert, B., Lyons, G., Simandl, B. K., Kuroiwa, A. and Buckingham, M. (1991). The apical ectodermal ridge regulates *Hox-7* and *Hox-8* gene expression in developing chick limb buds. *Genes Dev.* **5**, 2363-2374.

Rowe, D. A., Cairns, J. M. and Fallon, J. F. (1982). Spatial and temporal patterns of cell death in limb bud mesoderm after apical ectodermal ridge removal. *Dev. Biol.* **93**, 83-91.

Satokata, I. and Maas, R. (1994). Msx1 deficient mice exhibit cleft palate and abnormalities of craniofacial and tooth development. *Nat. Genet.* **6**, 348-356.

Satokata, I., Ma, L., Ohshima, H., Bei, M., Woo, I., Nishizawa, K., Maeda, T., Takano, Y., Uchiyama, M., Heaney, S. et al. (2000). Msx2 deficiency in mice causes pleiotropic defects in bone growth and ectodermal organ formation. *Nat. Genet.* **24**, 391-395.

Saunders, J. W., Jr (1948). The proximo-distal sequence of origin of the parts of the chick wing and the role of the ectoderm. *J. Exp. Zool.* **108**, 363-403.

Saunders, J. W., Jr and Gasseling, M. T. (1968). Ectoderm-mesenchymel interaction in the origins of wing symmetry. In *Epithelial-Mesenchymal Interactions* (ed. R. Fleischmajer and R. E. Billingham), pp. 78-97. Baltimore: Williams and Wilkins.

Sekine, K., Ohuchi, H., Fujiwara, M., Yamasaki, M., Yoshizawa, T., Sato, T., Yagishita, N., Matsui, D., Koga, Y., Itoh, N et al. (1999). *Fgf10* is essential for limb and lung formation. *Nat. Genet.* **21**, 138-141.

Shimeld, S. M., McKay, I. J. and Sharpe, P. T. (1996). The murine homeobox gene *Msx-3* shows highly restricted expression in the developing neural tube. *Mech. Dev.* **55**, 201-210.

Summerbell, D. (1974). A quantitative analysis of the effect of excision of the AER from the chick limb-bud. *J. Exp. Zool.* **32**, 651-660.

Sun, X., Mariani, F. V. and Martin, G. R. (2002). Functions of FGF signalling from the apical ectodermal ridge in limb development. *Nature* **418**, 501-508.

Tanaka, M., Shigetani, Y., Sugiyama, S., Tamura, K., Nakamura, H. and Ide, H. (1998). Apical ectodermal ridge induction by the transplantation of En-1-overexpressing ectoderm in chick limb bud. *Dev. Growth. Differ.* **40**, 423-429.

Tanaka, M., Cohn, M. J., Ashby, P., Davey, M., Martin, P. and Tickle, C. (2000). Distribution of polarizing activity and potential for limb formation in mouse and chick embryos and possible relationships to polydactyly. *Development* **127**, 4011-4021.

te Welscher, P., Fernandez-Teran, M., Ros, M. A. and Zeller, R. (2002). Mutual genetic antagonism involving GLI3 and dHAND prepatterns the vertebrate limb bud mesenchyme prior to SHH signaling. *Genes Dev*. **16**, 421-426.

Tickle, C. (2003). Patterning systems-from one end of the limb to the other. *Dev. Cell* **4**, 449-458.

Vainio, S., Karavanova, I., Jowett, A. and Thesleff, I. (1993). Identification of BMP-4 as a signal mediating secondary induction between epithelial and mesenchymal tissues during early tooth development. *Cell* **75**, 45-58.

Wang, C.-K. L., Omi, M., Ferrari, D., Cheng, H.-C., Lizarraga, G., Chin, H.-J., Upholt, W. B., Dealy, C. N. and Kosher, R. A. (2004). Function of BMPs in the apical ectoderm of the developing mouse limb. *Dev. Biol.* **269**, 109-122.

Wang, W., Chen, X., Xu, H. and Lufkin, T. (1996). *Msx3*: a novel murine homologue of the Drosophila msh homeobox gene restricted to the dorsal embryonic central nervous system. *Mech. Dev.* **58**, 203-215.

Yokouchi, Y., Sakiyama, J., Kameda, T., Iba, H., Suzuki, A., Ueno, N. and Kuroiwa, A. (1996). BMP-2/-4 mediate programmed cell death in chicken limb buds. *Development* **122**, 3725-3734.

Zeller, R. (2004). It takes time to make a pinky: Unexpected insights into how SHH patterns vertebrate digits. *Sci. STKE* **259**, pe53.

Zeller, R. and Duboule, D. (1997). Dorso-ventral limb polarity and origin of the ridge: on the fringe of independence? *BioEssays* **19**, 541-546.

Zhang, W., Behringer, R. R. and Olson, E. N. (1995). Inactivation of the myogenic bHLH gene MRF4 results in up-regulation of myogenin and rib anomalies. *Genes Dev.* **9**, 1388-1399.

Zhang, Y., Zhang, Z., Zhao, X., Yu, X., Hu, Y., Geronimo, B., Fromm, S. H. and Chen, Y. (2000). A new function of BMP4: dual role for BMP4 in regulation of Sonic hedgehog expression in the mouse tooth germ. *Development* **127**, 1431-1443.

Zhang, Z., Song, Y., Zhao, X., Zhang, X., Fermin, C. and Chen, Y. (2002). Rescue of the cleft palate in Msx-1 deficient mice by transgenic Bmp4 reveals a network of BMP and Shh signaling in the regulation of mammalian palatogenesis. *Development* **129**, 4135-4146.

Zou, H. and Niswander, L. (1996). Requirement for BMP signaling in interdigital apoptosis and scale formation. *Science* **272**, 738-741.

Zùniga, A., Haramis, A.-P. G., McMahon, A. P. and Zeller, R. (1999). Signal relay by BMP antagonism controls the SHH/FGF4 feedback loop in vertebrate limb buds. *Nature* **401**, 598-602.